Wing Box Optimization under Combined Shear and Bending

Donald H. Emero* and Leonard Spunt†
North American Aviation, Inc., Los Angeles, Calif.

A method is presented for determining the optimum proportions of a minimum weight multirib or multiweb wing box structure subjected to vertical shear and unidirectional bending moment. The optimization expressions are presented in general form to encompass any combination of cover and support structure for which individual efficiency equations are available. The optimum wing box design is determined by minimizing total structure weight, including the compression cover panel and appropriate substructure. The influence of minimum gage and fastening material can be included for the support structure. It is shown that the effect of vertical shear on the spacing of the webs is equally as important as the moment load in determining the minimum box weight. In a design example, three cover configurations are compared for both the multirib and multiweb structural concepts for a typical high aspect ratio wing. A table of 23 optimized wide column and compression panel cover concepts is presented, including the necessary design equations and graphs for any desired structural efficiency. An analysis for corrugated shear webs, optimized for simultaneous shear buckling, is included.

Nomenclature

A_c = former cap area
a, L = rib spacing
b = panel width
C = structural chord (Fig. 1)
$\bar{C}$ = $\frac{1}{2}(C_i + C_{i+1})$
C_r = stiffness coefficient
d = section depth
$\bar{d}$ = $\frac{1}{2}(d_i + d_{i+1})$
D = rigidity/ in.
E = modulus of elasticity
h = former depth
I = moment of inertia
K = buckling coefficient or Kth web in the interval
K_S = wide column shape factor
M = applied moment
n = number of stations i
n_1 = grid aspect ratio
N = number of spars or number of stringers
N_n = flexure induced crushing load
N_x = normal distributed load
N_{xy} = shear flow
P_{cr} = Euler critical load
r_{bw} = ratio of b_w/b_s
r_{tw} = ratio of t_w/t_s
R = radius of corrugation
S_K = length of Kth web
$\bar{t}_c$ = effective cover thickness defined such that area/panel $= \bar{t}_c \cdot b$
t_{FW} = thickness of former web
$\bar{t}_w$ = effective web thickness defined such that area/web $= \bar{t}_w \cdot d$
$\bar{t}_R$ = effective rib thickness defined such that area/rib $= \bar{t}_R \cdot C$
V = applied shear load
W_{ci} = cover weight in the ith interval
W_{Ri} = rib weight in the ith interval
W_{wi} = web weight in the ith interval
W_t = total weight of compression cover, webs, and ribs
W_i = interval weight of compression cover, webs, and ribs
$(X_k)_i$ = X coordinate of the Kth web, station i intercept
Y_i = length of the ith station interval
α = web efficiency equation exponent, or wide column dimensionless coefficient
β = cover efficiency equation exponent (panel failure), or wide column dimensionless coefficient
γ = cover efficiency equation exponent (wide column failure) or wide column dimensionless coefficient
γ_0 = taper angle as defined in Fig. 1
ϵ = efficiency factor
σ_c = cover compressive stress
σ_w = web shear stress
η_T = tangent modulus ratio
η_S = secant modulus ratio
$\bar{\eta}, \eta$ = general plasticity correction
ρ = material density
ρ_G = radius of gyration
λ = compression panel dimensionless coefficient
Ω = compression panel dimensionless coefficient
μ = Poisson's ratio
ϕ = corrugation angle

Subscripts

c = cover
cr = critical load
i = station interval
R = rib
w = web
m = referring to minimum gage
opt = optimum
a = load carrying

Introduction

The determination of an optimum structural arrangement of material to serve a required load-carrying function is generally considered an exercise in theoretical mechanics which produces the desired minimum weight configuration. In reality, the configuration ultimately selected as optimum for a given requirement is chosen only after due consideration of other factors, such as cost, producibility, inspectability, and the like. The goal of the structures engineer is to have available a means of evaluating many structurally optimized cross sections together with their respective cost-producibility-fabricability values. This would greatly facilitate early selection of a minimum number of candidate configurations in preliminary design situations, and narrow the focus of follow-on efforts to only those concepts that can reasonably be expected to result in an optimum design. In this regard, the objective of this report is to provide the fundamental optimization capabilities for multirib or multiweb wing box structures subjected to vertical shear and unidirectional bending moment.

Presented at the AIAA 6th Structures and Materials Conference, Palm Springs, Calif., April 5–7, 1965 (no preprint number; published in bound volume of preprints of the meeting); submitted April 12, 1965; revision received December 6, 1965. The authors express gratitude to R. M. Luhring and R. W. Falconer for their assistance in the preparation of this manuscript.
* Senior Structures Engineer, Structures Research.
† Structures Engineer, Structures Research.

Structural Weight Minimization

General Weight Equation

Web weight

From Fig. 1, the length of the Kth web, in the ith interval, can be expressed as follows:

$$S_K = \{Y_i^2 + [(X_k)_i - (X_k)_{i+1}]^2\}^{1/2} \quad (1)$$

where

$$(X_k)_i = (K - 1)b_i$$
$$(X_k)_{i+1} = (K - 1)b_{i+1} + Y_i \tan\gamma_0 \quad (2)$$

However, for evenly spaced webs

$$b_i = C_i/(N_i - 1) \quad (3)$$

combining Eqs. (1–3) and summing S_K for $K = 1$ to N, the total web weight for the station interval is as follows:

$$W_{wi} = \rho_w \bar{t}_{wi} \left(\frac{d_i + d_{i+1}}{2}\right) \sum_{K=1}^{N} S_K \quad (4)$$

where

$$S_K = \left\{Y_i^2 + \left[\frac{(K-1)}{(N-1)}(C_i - C_{i+1}) - Y_i \tan\gamma_0\right]^2\right\}^{1/2}$$

Cover weight

If it is assumed that wing depth will taper gradually, Sc can be approximated by Yi, therefore

$$W_{ci} = \rho_c \bar{t}_{ci}[(C_i + C_{i+1})/2]Y_i \quad (5)$$

where this represents the weight of the compression cover only.

Rib weight

Since chord and depth taper linearly, the rib weight is computed as the average weight times their total number as follows:

$$(W_{Ri})_{\text{ave}} = [(C_i + C_{i+1})/2][(d_i + d_{i+1})/2]\rho_R \bar{t}_{Ri} \quad (6)$$

The number of ribs are Y_i/a_i, where a_i is the rib separation in the ith interval. Therefore,

$$W_{Ri} = \tfrac{1}{4}\rho_R(C_i + C_{i+1})(d_i + d_{i+1})(Y_i/a_i)\bar{t}_{Ri} \quad (7)$$

where, if $\bar{t}_{Ri}$ is properly defined, Eq. (7) will hold for formers as well as for full depth ribs. The total weight of spars, ribs, and compression cover in the ith interval now can be written as the sum of Eqs. (4, 5, and 7)

$$W_i = \rho_w \bar{d} \bar{t}_{wi} \sum_{K=1}^{N} S_K + \rho_c Y_i \bar{C} \bar{t}_{ci} + \rho_R \bar{C} \bar{d} \left(\frac{Y_i}{a_i}\right) \bar{t}_{Ri} \quad (8)$$

where, for convenience, the following notation has been introduced:

$$\bar{C} = (C_i + C_{i+1})/2 \qquad \bar{d} = (d_i + d_{i+1})/2$$

Optimum Weight

Load and geometry

Equation (8) is derived from purely geometric considerations and makes no assumption as to the functional relation between geometry and load. In order to consider the variation of weight with N_i or a_i, relations must be found for $\bar{t}_{wi}$, $\bar{t}_{Ri}$, and $\bar{t}_{ci}$ in terms of load, substructure placement, and given geometry. The orientation of structure and load will be as shown in Fig. 1, where C_i, d_i, V_i, and M_i are assumed as fixed parameters at any given station.

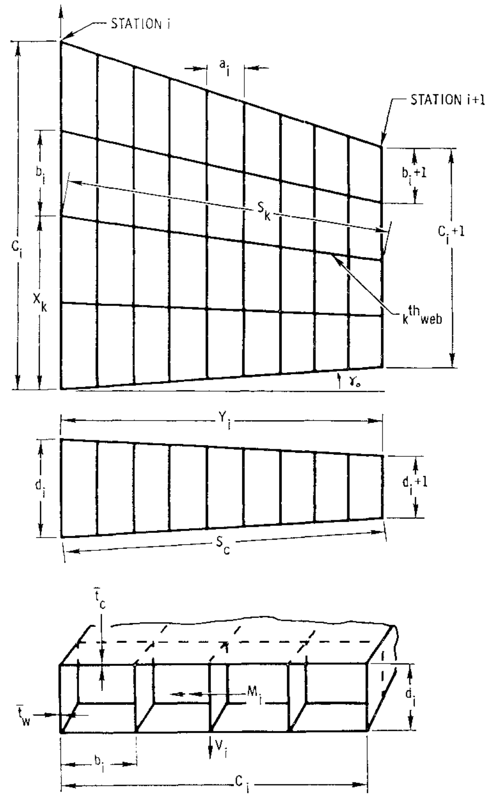

Fig. 1 Typical station interval and loads.

Multiweb Structures

Function of substructure

The webs will be designed on the basis of shear buckling with a minimum gage constraint as a lower bound on web thickness. In the past, stiffness and resistance to flexure-induced crushing has served as failure criteria in a pure moment analysis. In such analyses, however, the conclusion is that web gages computed from either strength of stiffness are too low to be considered practical,[1] and, as a consequence, shear load will be the governing factor in an actual web design. It has been found that, even when shear is low, a practical minimum gage requirement is several orders of magnitude larger than gages predicted from stiffness or strength.[2] Hence, shear buckling or minimum gage appears to be the most reasonable failure criterion in a minimum weight analysis.

In the multiweb analysis, the cover will fail as a simply-supported panel of high aspect ratio. It will be assumed that ribs, if any, have a fixed separation (a_i) and exist for reasons other than cover support. Tacit here, is the assumption that at optimum proportions the number of webs is sufficiently large, so that rib support can be neglected.

Web failure

The shear load V_i is assumed to divide uniformly to the N_i equally spaced webs, where

$$N_{xy} = V_i/(N_i d_i) \quad (9)$$

as the applied shear flow. The allowable shear flow can be related to effective thickness by assuming a generalized efficiency equation of the form

$$N_{xy}/(d_i \eta_w E_w) = \epsilon_w(\bar{t}_{wi}/d_i)^\alpha \quad (10)$$

where such an equation results from a minimum weight analysis of the particular element as shown in the appendix for the circular corrugated web. Combining Eqs. (9) and (10) and solving for $\bar{t}_{wi}$, we have

$$\bar{t}_{wi} = [(V_i d_i^{\alpha-2})/(\eta_w E_w \epsilon_w)]^{(1/\alpha)} N_i^{-(1/\alpha)} \quad (11)$$

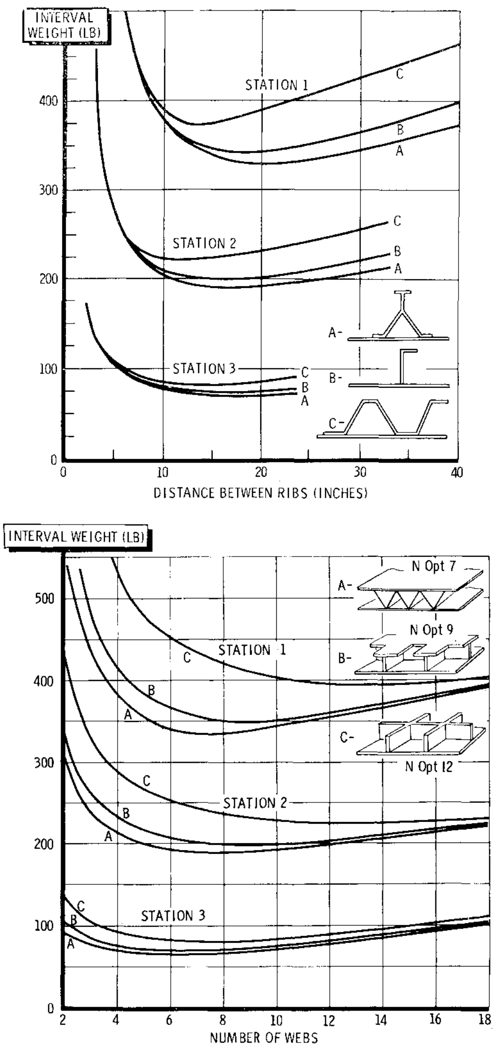

Fig. 2 Example weight vs substructure spacing graphs.

Cover failure

The cover will be assumed to carry the entire spanwise moment with bending stresses neglected in the webs. Obviously, this assumption is more reasonable for corrugated webs than for other types of constructions. The applied moment can therefore be split into the following equal and opposite cover loads:

$$N_x = M_i/(d_iC_i) \quad (12)$$

Again, a generalized efficiency equation is written for simultaneous buckling mode occurrence at the applied load

$$N_x/(b_i\eta_cE_c) = \epsilon_c(\bar{t}_{ci}/b_i)^\beta \quad (13)$$

Combining Eqs. (12) and (13) and recognizing that $b_i = C_i/(N_i - 1)$ yields

$$\bar{t}_{ci} = [(M_iC_i^{\beta-2})/(\eta_cE_c\epsilon_cd_i)]^{1/\beta}(N_i - 1)^{-[(\beta-1)/\beta]} \quad (14)$$

Optimum web placement

Substituting the expressions for $\bar{t}_{wi}$ and $\bar{t}_{ci}$ into the general weight equation, the interval weight becomes

$$W_i = \rho_w\bar{d}\left[\frac{V_id_i^{\alpha-2}}{\eta_wE_w\epsilon_w}\right]^{1/\alpha} N_i^{-(1/\alpha)} \sum_{K=1}^{Ni} S_K + \rho_cY_i\bar{C}\left[\frac{M_iC_i^{\beta-2}}{\eta_cE_c\epsilon_cd_i}\right]^{1/\beta}(N_i - 1)^{-[(\beta-1)/\beta]} + W_{Ri} \quad (15)$$

Since rib separation is assumed constant, Eq. (15) is a function of N_i only, and, consequently, for given materials, load and over-all geometry can be evaluated for any N_i. Two modes of variation on N will be considered. In the first, N_{opt} will be determined for each station interval independently, and, secondly, the total weight of all intervals will be minimized under the arbitrary constraint that N_i will be the same for all station intervals. The implication here is that the weight penalty associated with a fixed optimum number of webs for all intervals is small by virtue of the fact that interval weight is relatively insensitive to N (see Fig. 2). Differentiating the interval weight, Eq. (15), with respect to N_i, and after some algebraic manipulation, yields for $N_{i\text{opt}}$ the following implicit relation

$$\left[\frac{(N_i - 1)^{(2\beta-1)/\beta}}{N_i^{1/\alpha}}\right]_{\text{opt}} = \frac{\alpha(\beta - 1)\bar{C}\rho_c}{\beta(\alpha - 1)\bar{d}\rho_w} \times \left(\frac{M_iC_i^{\beta-2}}{\eta_cE_c\epsilon_cd_i}\right)^{1/\beta}\left(\frac{V_id_i^{\alpha-2}}{\eta_wE_w\epsilon_w}\right)^{-(1/\alpha)} \quad (16)$$

where NY_i has been substituted for ΣS_K. Such a substitution is tantamount to assuming all webs in the interval have the same length, equal to the interval length. This is done in order to simplify mathematical optimization; however, in a machine program this simplification is not needed since the program could compute weight for a range of N's and select the minimum. The mathematical optimization is presented here to show general trends. One fact, immediately evident from Eq. (16), is that the optimum number of webs depends in some manner on the ratio of moment to shear. This relation becomes clear if it is assumed that $(N - 1)$ can be approximated by N, whereby

$$(N_i)_{\text{opt}} \sim (M_i^\alpha/V_i^\beta)^{1/(2\alpha\beta-\alpha-\beta)} \quad (17)$$

and, consequently, it can be seen that shear, as well as moment, plays a critical role in the determination of the number of webs which minimize the total structural weight. In order to consider the case where N_{opt} is independent of station interval, the subscript on N in Eq. (15) is dropped, and W_i is summed over the n intervals, whereby total weight is obtained as follows:

$$W_T = \sum_{i=1}^{n}\left\{\rho_w\bar{d}\left[\frac{V_id_i^{\alpha-2}}{\eta_wE_w\epsilon_w}\right]^{1/\alpha} N^{-(1/\alpha)} \sum_{K=1}^{N} S_K + \rho_cY_i\bar{C} \times \left[\frac{M_iC_i^{\beta-2}}{\eta_cE_c\epsilon_cd_i}\right]^{1/\beta}(N - 1)^{-[(\beta-1)/\beta]} + W_{Ri}\right\} \quad (18)$$

Forming dW_T/dN we arrive at an expression similar to Eq. (16), except here a single value of N has been found such that total weight (for all intervals) is minimized.

$$\left[\frac{(N - 1)^{(2\beta-1)/\beta}}{N^{1/\alpha}}\right]_{\text{opt}} = \frac{\alpha(\beta - 1)\rho_c}{\beta(\alpha - 1)\rho_w}\sum_{i=1}^{n}\bar{C}Y_i \times \left[\frac{M_iC_i^{\beta-2}}{\eta_cE_c\epsilon_cd_c}\right]^{1/\beta} \Big/ \sum_{i=1}^{n}\bar{d}Y_i\left[\frac{V_id_i^{\alpha-2}}{\eta_wE_w\epsilon_w}\right]^{1/\alpha} \quad (19)$$

where, again, NY_i has replaced ΣS_K for mathematical expediency. Unlike Eq. (16), (19) also is independent on the station interval lengths as might be expected. This results from the fact that, by requiring a constant N, certain intervals must assume suboptimum N's; consequently, the size of these intervals plays an important role in the compromise between the interval N_{opt} and the entire wing N_{opt}. The critical dependence on shear again is noted.

Multirib Structures

Function of substructure

In the multirib analysis, rib separation is considered the optimized variable. The ribs themselves exist for support of the wide column cover and are designed to meet both stiffness and strength requirements. In addition, a minimum gage constraint can be established as a lower bound on rib thickness. There will be N webs, where N is considered a parameter and not an optimized variable. The webs are assumed to be placed such that they contribute negligible support to the wide column cover and exist to carry shear loads.

Cover failure

The same assumptions as stated in the multiweb analysis apply here, except that the cover is assumed to fail as a wide column, simply supported at the rib attachments. The applied cover loads again are given by Eq. (12), and the following generalized efficiency equation is assumed to predict the simultaneous mode wide column failure

$$N_x/(a_i\eta_c E_c) = \epsilon_c(\bar{t}_{ci}/a_i)^\gamma \tag{20}$$

Combining with Eq. (12) yields

$$\bar{t}_{ci} = [M_i/(d_iC_i\eta_cE_c\epsilon_c)]^{1/\gamma}\, a_i^{[(\gamma-1)/\gamma]} \tag{21}$$

as the required effective thickness in terms of rib spacing.

Rib failure

The applied loads, which the ribs must resist, are the flexure-induced crushing loads imposed by virtue of spanwise bending curvature. Seide and Eppler[3] showed that, in addition, certain stiffness requirements must be met in order that the idealized column strength of the compression panel can be attained. The ribs, therefore, must be designed for either strength or stiffness, whichever is critical.

Stiffness

The stiffness of an idealized rib (which neglects the effects of flanges) can be expressed in terms of rib effective thickness as[4]

$$\psi_{\text{rib}} = (E_R\bar{t}_{Ri})/d_i \tag{22}$$

The required stiffness, necessary to enforce nodes for wide column failure of the compression cover is

$$\psi_{\text{req}} = C_r[(E_cI_c)/(C_ia_i^3)] \tag{23}$$

where C_r is a stiffness parameter depending upon the ratio of of the flexural rigidity of the tension and compression panels. Assuming these to be equal, $C_r = 67.5$. For other values, refer to Ref. 4. The E_cI_c of the wide column cover panel can be found in terms of applied moment as follows:

$$P_{\text{cr}} = (\pi^2E_cI_c)/a_i^2 \tag{24}$$

but

$$P_{\text{cr}} = M_i/d_i \tag{25}$$

therefore

$$E_cI_c = (M_ia_i^2)/(\pi^2d_i) \tag{26}$$

combining this with Eqs. (22) and (23) we find $\bar{t}_{Ri}$ for sufficient stiffness

$$\bar{t}_{Ri} = [Cr/(\pi^2E_R)]M_i/(C_ia_i) \tag{27}$$

Strength

The ribs must possess sufficient strength to withstand wide column buckling under the applied crushing load, which can be easily shown to be

$$N_n = (2a_iN_x^2)/(\eta_SE_cd_i\bar{t}_{ci}) \tag{28}$$

Assume that an efficiency equation exists for the wide column rib configuration and predicts the allowable crushing load as follows:

$$N_n/(d_i\eta_RE_R) = \epsilon_R(\bar{t}_{Ri}/d_i)^\delta \tag{29}$$

substituting Eqs. (20) and (21) for N_x and $\bar{t}_{ci}$, respectively, into Eq. (28) and equating applied to allowable load yields $\bar{t}_{Ri}$ for sufficient strength.

$$\bar{t}_{Ri} = \left[\frac{2(\eta_cE_c\epsilon_c)^{1/\gamma}}{\eta_SE_cd_i^{2-\delta}\eta_RE_R\epsilon_R}\right]^{1/\delta}\left(\frac{M_i}{d_iC_i}\right)^{[(2\gamma-1)/(\gamma\delta)]} a_i^{1/(\delta\gamma)} \tag{30}$$

The required rib effective thickness must be the larger of Eqs. (27) and (30) to ensure sufficient stiffness and strength for the applied moment. It should be noted that any of the wide column concepts in Table 1 can be employed as full depth ribs, since all have the form of Eq. (29).

Partial depth ribs (formers)

The formers are designed to provide the stiffness required to create a simply-supported condition for the wide column cover panel. It is shown[5] that the required flexural rigidity can be expressed by

$$E_RI_R = 4\,(b_i/\pi)^4N_x/a_i \tag{31}$$

Substituting Eq. (12) for N_x, the required inertia is

$$I_R = 4/E_R(b_i/\pi)^4[M_i/(a_iC_id_i)] \tag{32}$$

If it is assumed that the former geometry can be represented by two cap areas separated by a web of depth h, the inertia provided will be

$$I_R = (A_ch^2/2) + (t_{FW}h^3/12) \tag{33}$$

Equating Eqs. (32) and (33) gives the required cap area

$$A_c = (2/h^2)\{(4/E_R)(b_i/\pi)^4[M_i/(a_iC_id_i)] - [(h^3t_{FW})/12]\} \tag{34}$$

If t_{FW} is constrained at minimum gage, a stationary value of the total former cross section can be found by virtue of the stiffness constraining relation, Eq. (34), and results in

$$h_{\text{opt}} = [48/(t_{FW}E_R)](b_i/\pi)^4[M_i/(a_iC_id_i)] - [(h^3t_{FW}/12)] \tag{35}$$

Since h must be bounded, as previously shown, by one-half the section depth, h_{opt} is seldom realistic, and, in general, a cap area A_c will be required. For use in weight calculations, an effective thickness can be defined for the former configuration as follows:

$$\bar{t}_{Ri} = [(2A_c)/d_i] + [(ht_{FW})/d_i] \tag{36}$$

Web failure

Equation (11) will dictate web effective thickness where N_i is now treated as a preassigned constant. Use of Eq. (11) also implies that any additional support supplied by rib attachment is ignored.

Optimum rib placement

For full depth ribs, the interval weight must be examined for a stationary value with respect to both stiffness and strength as rib design criteria. For any given a_i, the larger of rib effective thicknesses computed from strength or stiffness must be used in the final weight figure. With this in mind, we first write the total interval weight with stiffness dictating rib weight. By combining Eqs. (8, 21, and 27), it follows that

$$W_i = \rho_cY_i\bar{C}\left[\frac{M_i}{\eta_cE_c\epsilon_cd_iC_i}\right]^{1/\gamma} a_i^{(\gamma-1)/\gamma} + \rho_RY_i\bar{C}\bar{d}\frac{C_rM_i}{\pi^2E_RC_i}\,a_i^{-2} + W_{wi} \tag{37}$$

Table 1 Wide column concepts

THE FOLLOWING RELATIONS HOLD FOR ALL WIDE COLUMN CONFIGURATIONS EXCEPT AS NOTED IN THE TABLE.

$$\frac{N_x}{L\bar{\eta}E} = \epsilon\left(\frac{\bar{t}}{L}\right)^2$$

$$t_s = \frac{\bar{t}\left(1 + r_{bz}\right)}{\alpha} \qquad b_s = \left[\frac{N_x L^2}{\pi^2 \eta_T E\bar{t}} \; \frac{\alpha}{\gamma - \frac{\beta^2}{\alpha}}\right]^{1/2} \qquad \rho = b_s\left[\frac{\gamma - \frac{\beta^2}{\alpha}}{\alpha}\right]^{1/2}$$

$$b_i = r_{bi}\, b_s \qquad t_i = r_{ti}\, t_s$$

$$\eta_L = \left(\frac{E_T}{E}\right)^{1/2} \qquad \eta_T = \frac{E_T}{E} = \eta_G \qquad \bar{\eta} = \eta_T^{3/4}$$

CONFIGURATION	DESIGN CURVES	OPTIMUM VALUES	AUXILIARY RELATIONS	DIMENSIONLESS GEOMETRIC EXPRESSIONS
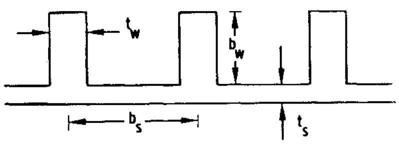 Integrally Stiffened	Ref 1	$\epsilon_{max} = 0.656$ $r_{bw} = 0.65$ $r_{tw} = 2.25$	$r_{bz} = 0$	$\alpha = 1 + r_{bw} r_{tw}$ $\beta = .5\, r_{bw}^2 r_{tw}$ $\gamma = .333\, r_{bw}^3 r_{tw}$
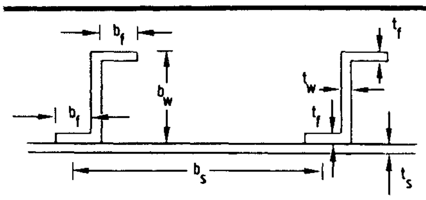 Zee Stiffened	Ref 1	$\epsilon_{max} = 0.911$ $r_{bw} = 0.87$ $r_{tw} = 1.06$	$r_{bf} = 0.3\, r_{bw}$ $r_{tf} = 1.0\, r_{tw}$ $r_{bz} = 0$	$\alpha = 1 + 1.6\, r_{bw} r_{tw}$ $\beta = .8\, r_{bw}^2 r_{tw}$ $\gamma = .633\, r_{bw}^3 r_{tw}$
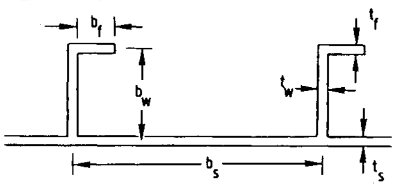 Integral Zee	Fig. 3	$\epsilon_{max} = 1.03$ $r_{bw} = 1.0$ $r_{tw} = 1.0$	$r_{bf} = 0.3\, r_{bw}$ $r_{tf} = 1.0\, r_{tw}$ $r_{bz} = 0$	$\alpha = 1 + 1.3\, r_{bw} r_{tw}$ $\beta = .8\, r_{bw}^2 r_{tw}$ $\gamma = .633\, r_{bw}^3 r_{tw}$
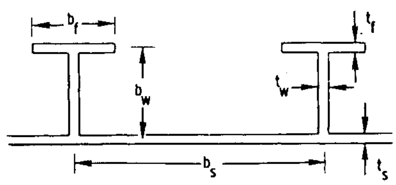 Integral Tee	Fig. 3	$\epsilon_{max} = 1.00$ $r_{bw} = 0.80$ $r_{tw} = 0.70$	$r_{bf} = 0.6\, r_{bw}$ $r_{tf} = 1.0\, r_{tw}$ $r_{bz} = 0$	$\alpha = 1 + 1.6\, r_{bw} r_{tw}$ $\beta = 1.1\, r_{bw}^2 r_{tw}$ $\gamma = .933\, r_{bw}^3 r_{tw}$

and, forming $dW_i/da_i = 0$, yields

$$(a_i)_{opt} = \left[\frac{2\bar{d}C_r\gamma\rho_R(\eta_c E_c\epsilon_c)^{1/\gamma}}{\pi^2(\gamma - 1)\rho_c E_R}\right]^{\gamma/(3\gamma-1)} \times \left(\frac{M_i d_i^{1/(\gamma-1)}}{C_i}\right)^{[(\gamma-1)/(3\gamma-1)]} \tag{38}$$

as the optimum rib spacing if stiffness is critical. Writing the interval weight with strength governing rib thickness requires the combination of Eqs. (8, 21, and 30) with the result

$$W_i = \rho_c Y_i \bar{C}\left[\frac{M_i}{\eta_c E_c \epsilon_c d_i C_i}\right]^{1/\gamma} a_i^{(\gamma-1)/\gamma} + \rho_R Y_i \bar{C}\bar{d}\left[\frac{2(\eta_c E_c\epsilon_c)^{1/\gamma}}{\eta_s E_c d_i^{2-\delta}\eta_R E_R \epsilon_R}\right]^{1/\delta}\left(\frac{M_i}{C_i d_i}\right)^{[(2\gamma-1)/(\delta\gamma)]} + W_{wi} \tag{39}$$

Table 1 continued

CONFIGURATION	DESIGN CURVES	OPTIMUM VALUES	AUXILIARY RELATIONS	DIMENSIONLESS GEOMETRIC EXPRESSIONS
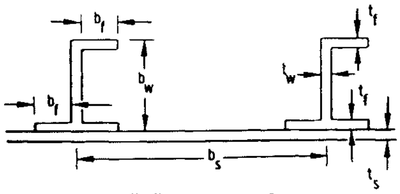 "J" Stiffened	Fig. 3	$\epsilon_{max} = 0.793$ $r_{bw} = 0.85$ $r_{tw} = 0.79$	$r_{bf} = 0.3\, r_{bw}$ $r_{tf} = 1.0\, r_{tw}$ $r_{bz} = 0$	$\alpha = 1 + 1.9\, r_{bw} r_{tw}$ $\beta = .8\, r_{bw}^2 r_{tw}$ $\gamma = .633\, r_{bw}^3 r_{tw}$
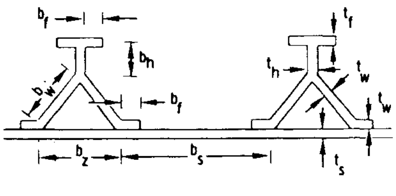 Straight Y-Tee Stiffened	Ref 8	$\epsilon_{max} = 1.23$ $r_{bw} = 0.90$ $r_{tw} = 0.90$	$r_{bh} = .938\, r_{bw}$ $r_{th} = 1.06\, r_{tw}$ $r_{bf} = .348\, r_{bw}$ $r_{tf} = 2.125\, r_{tw}$ $r_{bz} = 1.04\, r_{bw}$	$\alpha = 1 + r_{bz} + 5.17\, r_{bw} r_{tw}$ $\beta = 4.83\, r_{bw}^2 r_{tw}$ $\gamma = 7.07\, r_{bw}^3 r_{tw}$
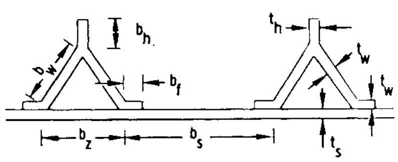 Straight Y-Stiffened	Ref 8	$\epsilon_{max} = 0.79$ $r_{bw} = 0.96$ $r_{tw} = 0.96$	$r_{bh} = .346\, r_{bw}$ $r_{th} = 1.06\, r_{tw}$ $r_{bf} = .348\, r_{bw}$ $r_{bz} = 1.04\, r_{bw}$	$\alpha = 1 + r_{bz} + 3.06\, r_{bw} r_{tw}$ $\beta = 1.23\, r_{bw}^2 r_{tw}$ $\gamma = .865\, r_{bw}^3 r_{tw}$
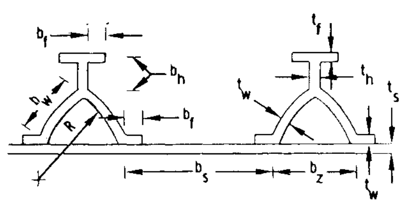 Curved Y-Tee Stiffened	Ref 8	$\epsilon_{max} = 1.23$ $r_{bw} = 0.90$ $r_{tw} = 0.90$	$r_{bh} = .938\, r_{bw}$ $r_{th} = 1.125\, r_{tw}$ $r_{bf} = .348\, r_{bw}$ $r_{tf} = 2.125\, r_{tw}$ $r_{bR} = .938\, r_{bw}$ $r_{bz} = 1.04\, r_{bw}$	$\alpha = 1 + r_{bz} + 5.31\, r_{bw} r_{tw}$ $\beta = 5.13\, r_{bw}^2 r_{tw}$ $\gamma = 7.58\, r_{bw}^3 r_{tw}$
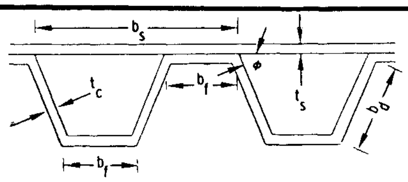 Trap. Corr. Semisandwich	Fig. 4	$\epsilon_{max} = .685$ $m = b_f/b_d = 0.18$ $\phi = 70°$	$r_{tc} = \left(\frac{4}{K_1}\right)^{1/2} r_{bd}$ $r_{bd} = \frac{1}{2(m + \cos\phi)}$ $r_{bz} = 0$ K_1 (Ref 8)	$\alpha = 1 + \frac{m+1}{K_1^{1/2}(m+\cos\phi)^2}$ $\beta = 4\frac{(m+1)\sin\phi}{K_1^{1/2}(m+\cos\phi)^3}$ $\gamma = \frac{(m+.667)\sin^2\phi}{8K_1^{1/2}(m+\cos\phi)^4}$
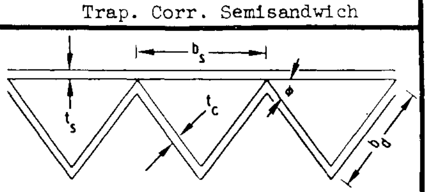 Truss Core Semisandwich		$\epsilon_{max} = .686$ $m = b_f/b_d = 0$ $\phi = 65°$		

and, forming $dW_i/da_i = 0$, we arrive at

$$(a_i)_{opt} = \left[\frac{(\delta\gamma - 1)\rho_R}{\delta(\gamma - 1)\rho_c} \times \frac{(2)^{1/\delta}\bar{d}(\eta_c E_c \epsilon_c)^{[(1+\delta)/(\delta\gamma)]}}{(\eta_S E_c d_i^{2-\delta}\eta_R E_R \epsilon_R)^{1/\delta}}\right]^{[(\gamma\delta)/(2\gamma\delta - \delta - 1)]} \quad (40)$$

as the optimum rib spacing if strength is critical. The larger of the $\bar{t}_R$'s using Eq. (27) and (30), will dictate the final design. In such a comparison, the rib thickness also can be conveniently checked against a minimum gage requirement. Optimum rib spacing also can be considered for the case where formers are used. By combining Eqs. (34) and (36), the former effective thickness can be expressed as

$$\bar{t}_{Ri} = [16/(d_i h^2 E_R)](b_i/\pi)^4[M_i/(d_i a_i C_i)] + (2h/3d_i)t_{FW} \quad (41)$$

and substituting into Eq. (8)

Table 1 continued

CONFIGURATION	DESIGN CURVES	OPTIMUM VALUES	AUXILIARY RELATIONS	DIMENSIONLESS GEOMETRIC EXPRESSIONS
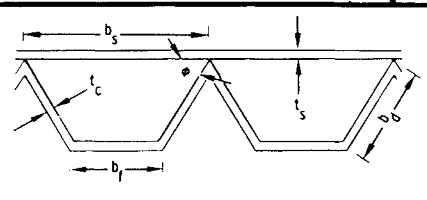 Semitrap. Corr. Semisandwich	Fig. 4	$\epsilon_{max} = 0.72$ $m = b_f/b_d = 0.65$ $\phi = 75°$ K_1 (Ref 7)	$r_{tc} = \left(\frac{4}{K_1}\right)^{1/2} r_{bd}$ $r_{bd} = \frac{1}{m+2\cos\phi}$ $r_{bz} = 0$	$\alpha = 1 + \frac{2(m+2)}{K_1^{1/2}(m+2\cos\phi)^2}$ $\beta = \frac{2(m+1)\sin\phi}{K_1^{1/2}(m+2\cos\phi)^3}$ $\gamma = \frac{2(m+.667)\sin^2\phi}{K_1^{1/2}(m+2\cos\phi)^4}$
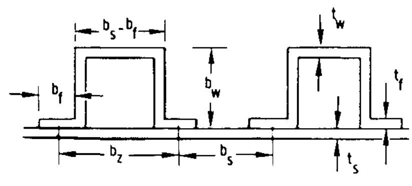 Hat Section Stiffened	Fig. 3	$\epsilon_{max} = .928$ $r_{bw} = 1.0$ $\frac{b_f}{b_w} = 0.3$ K (Ref 8)	$r_{bf} = \frac{b_f}{b_w} r_{bw}$ $r_{tw} = \frac{2(1-r_{bf})}{K^{1/2}}$ $r_{tf} = r_{tw}$ $r_{bz} = 1.0$	$\alpha = 2 + r_{tw}(1 + 2r_{bw} + r_{bf})$ $\beta = r_{bw} r_{tw}(1 - r_{bf} + r_{bw})$ $\gamma = r_{bw}^2 r_{tw}(1 - r_{bf} + .67 r_{bw})$
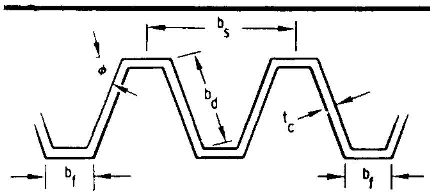 Trapezoidal Corrugation	Fig. 4	$\epsilon_{max} = 1.60$ $m = b_f/b_d = 0.85$ $\phi = 60°$	$t_c = t_s$ $r_{bd} = \frac{1}{2(m+\cos\phi)}$ $r_{bz} = 0$	$\alpha = 2r_{bd}(m+1)$ $\beta = r_{bd}^2 (m+1)\sin\phi$ $\gamma = r_{bd}^3 (m+.667)\sin^2\phi$
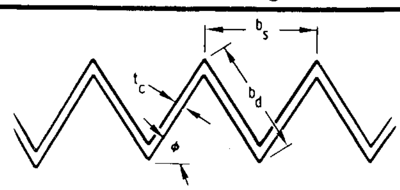 Truss Core Corrugation		$\epsilon_{max} = 1.15$ $m = b_f/b_d = 0$ $\phi = 45°$		
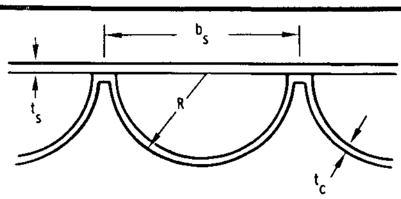 Semicircle Corr. Semisandwich	Fig. 4	$\epsilon_{max} = .706$ $r_{tc} = 0.23$	$\frac{R}{b_s} = 0.50$ $b_s = 5.45 \frac{t_s^*}{r_{tc}}$	$\alpha = 1 + 1.57 r_{tc}$ $\beta = .5 r_{tc}$ $\gamma = .196 r_{tc}$
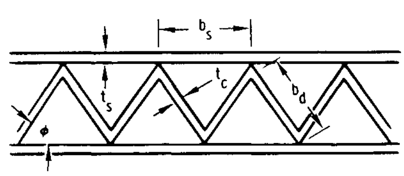 Truss Core Sandwich	Ref 1	$\epsilon_{max} = .605$ $r_{tc} = 0.92$ $\phi = 62°$	* EXCEPTIONS TO BASIC EQUATIONS $t_s = \frac{\bar{t}}{2 + (r_{tc}/\cos\phi)}$ * $b_s = 0.95 t_s \left[\frac{\bar{t} K_x \eta_T^{1/2} E}{N_x}\right]^{1/2}$ * $b_d = \frac{b_s}{2\cos\phi}$ $\bar{\eta} = \left(\frac{2\eta_T^{3/2}}{1+\eta_T}\right)^{1/2}$ *	

$$W_i = \rho_c Y_i \bar{C}\left[\frac{M_i}{\eta_c E_c \epsilon_c d_i C_i}\right]^{1/\gamma} a_i^{(\gamma-1)/\gamma} \times \rho_R \bar{C}\bar{d}\,\frac{Y_i}{a_i}\left[\frac{16}{d_i h^2 E_R}\left(\frac{b_i}{\pi}\right)^4 \frac{M_i}{d_i C_i a_i} + \frac{2h}{3d_i} t_{FW}\right] + W_{wi} \quad (42)$$

A minimum in Eq. (42) cannot be readily found through differentiation. It is recommended that a computer solution utilizing a discretely varying rib spacing be used. The use of formers suggests multiple spars, since the stiffness requirement varies as the fourth power of b_i.

Tables of optimized wide column and compression panel concepts are presented in this paper. Each concept has been optimized for simultaneous local and general instability failure, using the established methods of optimum design.[6–8] The efficiency equations shown in the tables are of the same format as Eqs. (13) and (20), and can be used directly in the wing box optimization analysis.

Sample Solution

A high aspect ratio wing box has been analyzed for optimum geometry under the imposed shear and moment loads noted in Table 2. The station interval was 100 in., shear webs were 60° arc corrugations, i.e., $\phi = 60°$, $\epsilon_w = 1.05$, and the material was titanium 8Al-1Mo-1V at room temperature.

Multirib Wing Box

The following cover configurations were employed: 1) y-tee stiffened skin, 2) integral zee stiffened skin, and 3) trapezoidal corrugation stiffened skin. The rib configuration was trapezoidal corrugation (no skin). The efficiency values (maximum) were taken directly from Table 1. Figure 2 shows interval weight as a function of rib separation for a two-spar configuration. Note that, at optimum proportions, wide column analysis for the cover is justified. In fact, the cover aspect ratio also would be small for a three- or four-spar configuration. In particular, the aspect ratio at all stations is approximately 0.5 for a four-spar box. A minimum gage constraint of 0.015 in. was employed for both the spar and rib, and cap weight also was included. This had the effect of creating a steeper ascent, to the right of optimum spacing, than that which would be predicted from Eqs. (37) and (39). Note that the three concepts of each station converge toward a common weight at the lower rib spacing values, where cover stresses are approaching compressive yield.

Multiweb Wing Box (No Ribs)

The following cover configurations were employed: 1) truss core sandwich, 2) 0°–90° tee-flanged grid, and 3) 0–°90° unflanged grid. The efficiency values were taken directly from Table 3. A graphical representation of the solution for minimum weight is shown in Fig. 2, where station weight has been plotted vs the number of webs. A minimum gage constraint for the shear webs of 0.015 in. was employed, and spar cap material was added to provide a more realistic appraisal. The graphs for each station are seen to present a wide range of spar spacings for which the station weight is minimum. The inclusion of fastener clip weights, etc., would narrow this range somewhat, but the analysis, as shown, provides a good preliminary design comparison among the concepts selected. The analysis for the optimum wing weight for a fixed number of spars along the wing length, Eq. (19), indicated the arrangements shown in Table 4. An inspection of Fig. 2 at each station for a particular structural concept will reveal that the station N optimum does not significantly differ from the optimum fixed number of spars. The graphs also indicate that, as spars are spaced closer together, the three concepts converge toward a common weight value at each station. This results from the high stress levels at which the concepts are operating, i.e., at or near compressive yield for the material.

Also noteworthy in this example is that the lightest of each of the configurations, multiweb and multirib, at any station indicates weights that are comparable. In this regard, a selection can be based on a cost-producibility comparison of the concepts, or other practical design considerations.

Figures 3–5 present efficiency curves associated with Tables 1 and 2.

Table 2 Analysis of a high aspect wing box under the imposed shear and moment loads

Station	Moment, in.-lb × 10⁶	Shear, lb × 10³	N_x, lb/in.	Chord, in.	Depth, in.
1	52.5	184.0	14,100	120.0	31.0
2	20.9	128.0	9,500	92.0	24.0
3	3.0	48.0	2,720	65.0	17.0
4	0	0	0	37.0	10.0

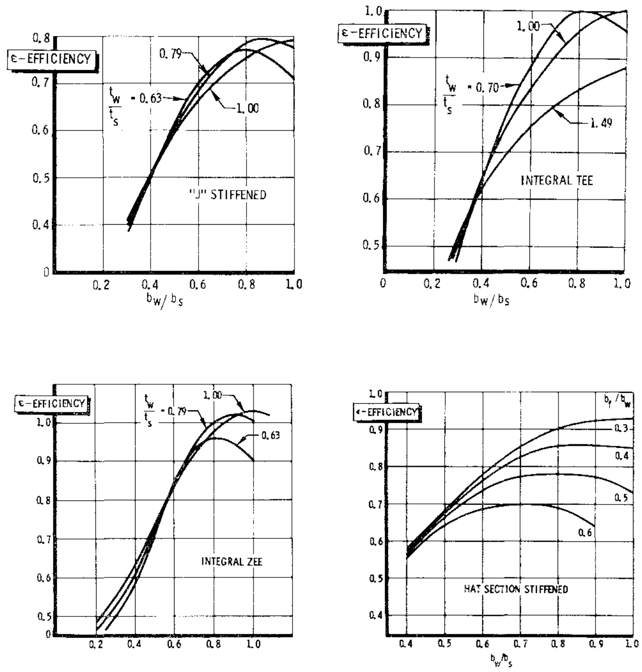

Fig. 3 Wide column efficiency curves.

Conclusions

The weight minimization expressions and optimization tables presented will provide the analytical means for determining favorable structural concepts for preliminary wing box designs. It has been shown that shear as well as moment plays a critical role in the determination of the number of webs that minimize total structural weight. The formulation for optimization of cover panel concepts and substructure, and for total weight minimization, has been presented in general form for simplicity in programming for digital computer solution. In the example solution, graphical representations of computer data have been presented to illustrate the analytical results. The relative flatness of the graphs indicates that some latitude in substructure spacing to meet practical design considerations is entirely feasible. The inclusion of minimum gage

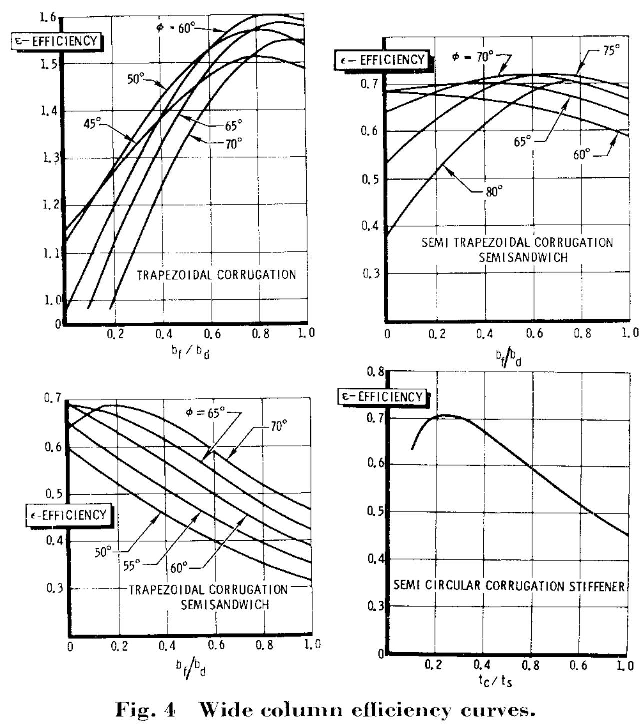

Fig. 4 Wide column efficiency curves.

Table 3 Compression panel concepts

EQUATIONS APPLICABLE TO CONCEPTS 1, 2

$$\frac{N_x}{b\,\bar{\eta}\,E} = \epsilon\left(\frac{\bar{t}}{b}\right)^{exp.} \qquad \bar{\eta} = \eta_T^{3/4}$$

$$b_s = b/N \qquad b_w = r_{bw}\,b_s \qquad b_f = r_{bf}$$

$$T_s = \frac{b_s\,(\bar{t}/b)\,N}{1 + \dfrac{C_1\,(N-1)\,r_{bw}^2}{N}} \qquad t_w = C_2\,r_{bw}\,t_s \qquad t_f = r_{tf}\,t_s$$

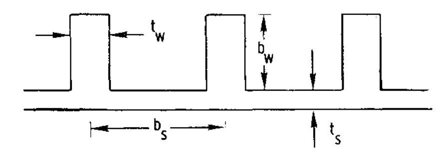 1. Integrally Stiffened	Ref 1	$\epsilon_{max} = 0.97$ exp. $= 2.38$ $C_1 = C_2 = 2.828$ $r_{bf} = 0$ $r_{tf} = 0$
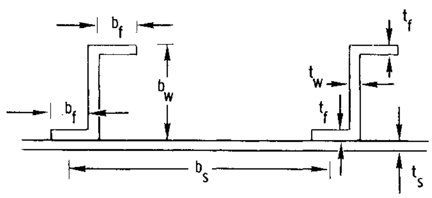 2. Zee Stiffened	Ref 1	$\epsilon_{max} = 1.03$ exp $= 2.36$ $C_1 = 1.707$ $C_2 = 1.0$ $r_{bf} = .3535\,r_{bw}$ $r_{tf} = r_{bw}$

EQUATIONS APPLICABLE TO CONCEPTS 3,4

$$\frac{N_x}{b\,\bar{\eta}\,E} = \epsilon\left(\frac{\bar{t}}{b}\right)^{2}$$

$$b_s = 0.95\,t_s\left[\frac{\bar{t}\,K_x\,\eta_T^{1/2}\,E}{N_x}\right]^{1/2} \qquad t_s = \frac{\bar{t}}{C_1 + (r_{tc}/\cos\phi)}$$

$$b_d = b_s/2\cos\phi \qquad \bar{\eta} = \left(\frac{2\,\eta_T^2}{1+\eta_T}\right)^{1/4} \qquad t_c = r_{tc}\,t_s$$

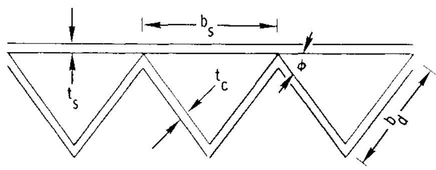 3 Truss Core Semisandwich	Ref 1	$\epsilon_{max} = 0.59$ r_{tc} (optimum) $= 0.49$ ϕ (optimum) $= 47.5°$ $C_1 = 1.0$
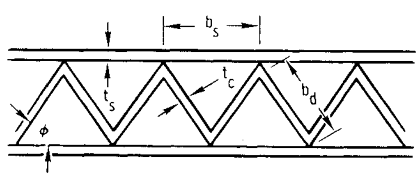 4 Truss Core Sandwich	Ref 1	$\epsilon_{max} = 1.108$ r_{tc} (optimum) $= 0.83$ ϕ (optimum) $= 60°$ $C_1 = 2.0$

Table 3 continued

EQUATIONS APPLICABLE TO CONCEPTS 5, 6, 7

$$\frac{N_x}{b\,\bar{\eta}\,E} = \epsilon\left(\frac{\bar{t}}{b}\right)^2$$

$$t_s = \bar{t}/\Omega \qquad b_s = 1.90\,t_s\left[\frac{\eta_T^{1/2}\,E\,t_s\,\lambda}{N_x}\right]^{1/2}$$

$$t_a = \lambda\,t_s$$

$$t_w = r_{tw}\,t_s \qquad b_w = r_{bw}\,b_s$$

$$t_f = r_{tw}\,t_s \qquad b_f = r_{bf}\,b_s$$

$$\bar{\eta} = \left[\eta_T^{1/2}\left(\frac{\eta_s + 3\eta_T}{4}\right)\right]^{1/2}$$

CONFIGURATION	DESIGN CURVES	OPTIMUM VALUES	AUXILIARY RELATIONS	DIMENSIONLESS GEOMETRIC EXPRESSIONS
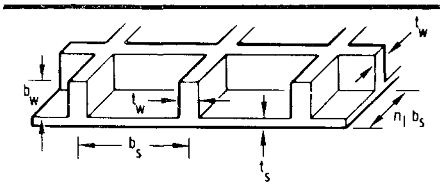 5 0° - 90° Unflanged Grid	Fig. 5	$\epsilon_{max} = .502$ $r_{bw} = 0.6$ $n_l = 4$	$r_{tw} = \frac{2}{k_w^{1/2}} r_{bw}$ $r_{bf} = 0$ $r_{tf} = 0$	$\lambda = 1 + r_b r_t$ $\Omega = 1 + r_b r_t \frac{n_l + 1}{n_l}$
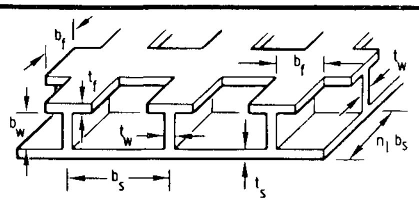 6 0° - 90° Tee-Flanged Grid	Fig. 5	$\epsilon_{max} = .88$ $r_{bw} = .775$ $n_l = 4$	$r_{tw} = r_{bw}$ $r_{bf} = 0.6\,r_{bw}$ $r_{tf} = r_{tw}$	$\lambda = 1 + 1.6\,r_b r_t$ $\Omega = 1 + 1.6\,r_b r_t \frac{n_l + 1}{n_l}$
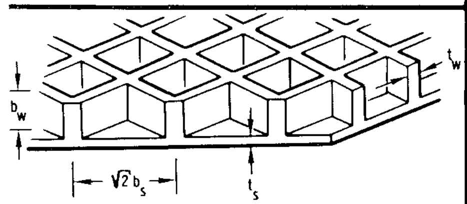 7 ± 45° Unflanged Grid	Fig. 5	$\epsilon_{max} = .628$ $r_{bw} = .75$	$r_{tw} = \frac{1.39}{k_w^{1/2}} r_{bw}$ $r_{bf} = 0$ $r_{tf} = 0$	$\lambda = 1 + .5\,r_{bw} r_{tw}$ $\Omega = 1 + 2\,r_{bw} r_{tw}$

constraints and cap material for the substructure provides a more realistic appraisal of the optimum substructure spacing.

Appendix

Corrugated Shear Web

Since bending stresses in the webs have been assumed negligible throughout this study, the corrugated shear web adheres to this assumption while providing inherent stability for flexure-induced crushing loads. The geometry and load are as shown in Fig. 6. A simply-supported condition will be assumed for both local and general modes, where simultaneous occurrence of these modes will be taken as the criterion for minimum weight.

General Stability

Timoshenko[9] presents the following expression for the critical buckling load:

$$(N_{xy})_{cr} = 4K[(D_1D_2^3)^{1/4}/d^2] \tag{A1}$$

The buckling coefficient K depends on θ and ψ, where

$$\theta = (D_1D_2)^{1/2}/D_3 \qquad \psi = (d/a)(D_1/D_2)^{1/2}$$

For an infinitely long plate, $\psi = 0$, and since normally $(D_1D_2)^{1/2} \gg D_3$, it can be considered that $1/\theta$ is approximately zero. Under these conditions $K = 8.0$. (For other values of K, see Ref. 9.) Since the value of K does not enter into the optimization of the corrugation angle, it will be left unspeci-

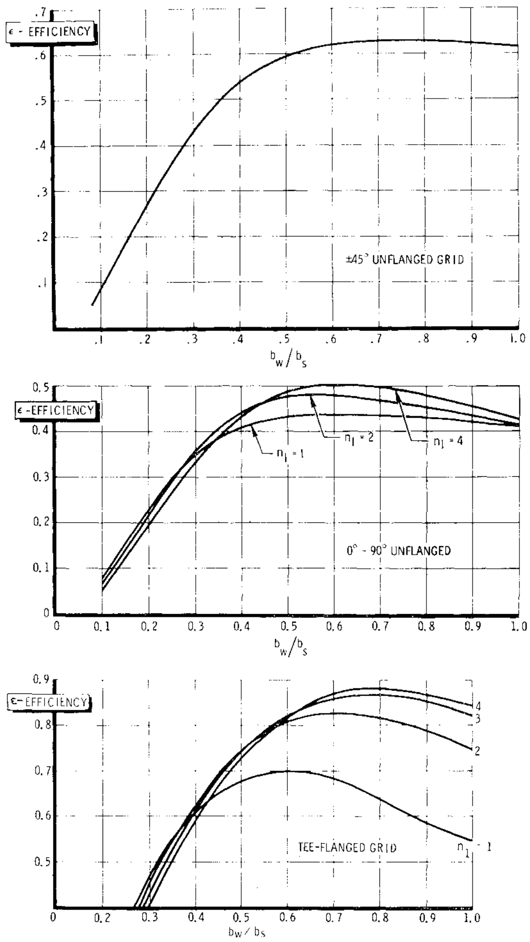

Fig. 5 Waffle grid efficiency curves.

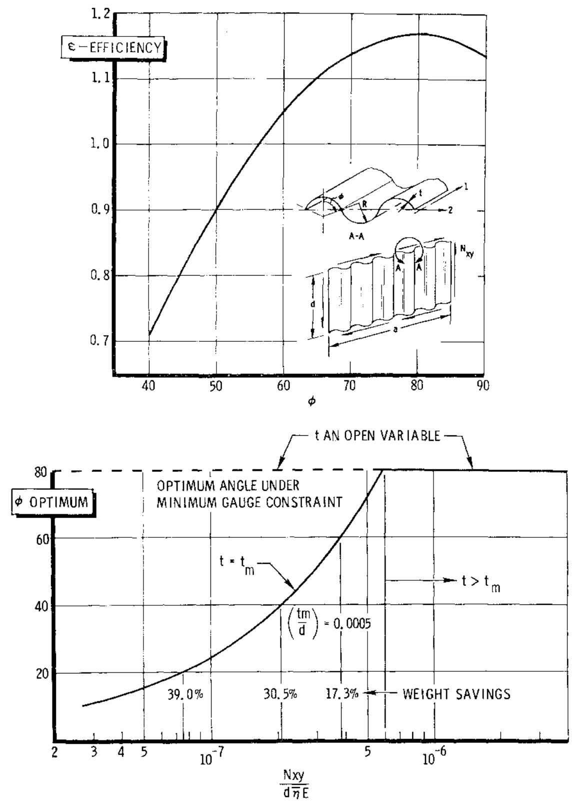

Fig. 6 Corrugated shear web curves.

fied. D_1 and D_2 can be expressed as follows:

$$D_1 = \{(Et^3)/[12(1 - \mu_x\mu_y)]\}(\sin\phi/\phi) \quad (A2)$$

$$D_2 = (EI_2)/(1 - \mu_x\mu_y) \quad (A3)$$

Where, in Eq. (A2), $(\sin\phi)/\phi$ is a reduction factor that accounts for curvature.[10] I_2 can be written in terms of R, t, and ϕ as follows:

$$I_2 = \rho_G{}^2\bar{t} \quad (A4)$$

where radius of gyration ρ_G, can be expressed as

$$\rho_G = R\left(\frac{1}{2} - \frac{3}{4}\frac{\sin 2\phi}{\phi} + \cos^2\phi\right)^{1/2} \quad (A5)$$

and

$$\bar{t} = (\phi/\sin\phi)t \quad (A6)$$

Combining Eqs. (A1–A6) yields

$$(N_{xy})_{cr} = 0.76\eta_l KE\,\frac{t^{3/2}R^{3/2}}{(1 - \mu_x\mu_y)} \times \left[\left(\frac{\phi}{\sin\phi}\right)^{2/3}\left(\frac{1}{2} - \frac{3}{4}\frac{\sin 2\phi}{\phi} + \cos^2\phi\right)\right]^{3/4} \quad (A7)$$

Table 4 Analysis for the optimum wing weight for a fixed number of spars along the wing length

Configuration	N optimum
Truss core sandwich	7
0°–90° tee-flanged grid	9
0°–90° unflanged grid	12

$\eta_l = 0.83\eta_S + 0.17\eta_T$ (Stowell[11] inelastic correction factor). Dividing by t and assuming that $\mu_x\mu_y = 0$ yields

$$\sigma_{wG} = 0.76\eta_l KE\left(\frac{t}{d}\right)^2\left(\frac{2R}{t}\right)^{3/2} f(\phi) \quad (A8)$$

where

$$f(\phi) = \left[\left(\frac{\sin\phi}{\phi}\right)^{2/3}\left(\frac{1}{2} - \frac{3}{4}\frac{\sin 2\phi}{\phi} + \cos^2\phi\right)\right]^{3/4}$$

Local stability

The expression used to predict the local shear buckling will be a semiempirical equation developed at North American Aviation, Los Angeles Division. Exhaustive testing has shown that this expression closely fits available test data and can be considered independent of ϕ for the range $20° < \phi < 90°$

$$\sigma_{wL} = 1.55\eta_T{}^{1/2}E(t/2R)^{3/2} \quad (A9)$$

Optimum corrugation angle

Equating the expression for general and local instability, Eqs. (A8) and (A9), and after some algebraic manipulation yields the following efficiency equation representation:

$$(N_{xy})/(\eta_w Ed) = [1.088K^{1/2}(\sin\phi/\phi)^2\{f(\phi)\}^{1/2}](\bar{t}/d)^2 \quad (A10)$$

$$\eta_w = \eta_l{}^{1/2}\eta_T{}^{1/4}$$

where it can be seen that

$$\epsilon = 1.088K^{1/2}(\sin\phi/\phi)^2[f(\phi)]^{1/2} \quad (A11)$$

is a function of ϕ only. Figure 6 shows that efficiency attains a maximum for $\phi = 80°$, where, if K is taken as equal to 8.0, $\epsilon_{max} = 1.17$. In the sample solution presented, 60° arc corrugated webs were employed because of fabrication considerations that render it a more desirable structure. At $\phi =$

60° the efficiency is reduced to $\epsilon = 1.05$ with a corresponding weight increase of 2.0% over the optimum.

By combining Eqs. (A9) and (A10) the corrugation radius index, for $K = 8.0$ can be expressed as follows:

$$(2R/d) = 1.34[\sin\phi/(\phi\epsilon^{1/2})]^{5/3}\eta_T^{1/3}\eta_w^{-5/6}(N_{xy}/Ed)^{1/6} \quad (A12)$$

The skin thickness can be obtained from Eq. (A6).

Optimum angle under minimum gage constraint

It was previously shown that efficiency can be maximized independently of load intensity. This is only true, however, if the skin gage is an open variable, ie., free to assume any positive real number. If it is assumed that t is constrained at t_m, Eq. (A10) becomes

$$(N_{xy})/(\eta_w Ed) = [1.088K^{1/2}\{f(\phi)\}^{1/2}](t_m/d)^2 \quad (A13)$$

and, consequently

$$\{f(\phi)\}^{1/2} = 0.92\{[N_{xy}/(\eta_w Ed)]/[K^{1/2}(t_m/d)^2]\} \quad (A14)$$

is load dependent if the efficiency equation is still to be satisfied. Equation (A14) can be evaluated graphically as a function of load index with t_m/d as a parameter. Figure 6 shows a typical parametric curve with percentage weight savings indicated over the 80° configuration with t constrained at t_m.

References

[1] Crawford, R. F. and Burns, A. B., "Strength efficiency, and design data for beryllium structures," Aeronautical Systems Div. TR 61-692 (February 1962).

[2] Spunt, L., "Preliminary optimization and evaluation of multiweb and multirib wings," North American Aviation, Inc., Rept. NA-64-645, pp. 25–28 (August 1964).

[3] Seide, P. and Eppler, J., "The buckling of parallel simply supported tension and compression members connected by elastic deflection springs," NACA TN 1823 (1955).

[4] Berke, L. and Vergamini, P., "Design optimization procedures and experimental program for box beam structures," Wright Air Development Div. TR 60-149, Vol. 1, pp. 95 (1960).

[5] Gerard, G., "Handbook of structural stability part V—Compressive strength of flat stiffened panels," NACA TN 3785, pp. 35 (August 1957).

[6] Shanley, F. R., "Principles of structural design for minimum weight," J. Aeronaut. Sci. **16**, 133–149 (1949).

[7] Needham, R. A., "Optimum design of shell structures," In-Plant Lecture Notes, Lockheed Missile and Space Div., Sunnyvale, Calif. (1961).

[8] Emero, D. H. and Spunt, L., "Optimization of multirib and multiweb wing box structures under shear and moment loads," *AIAA 6th Structures and Materials Conference* (American Institute of Aeronautics and Astronautics, New York, 1965), pp. 330–353.

[9] Timoshenko, S., *Theory of Elastic Stability* (McGraw-Hill Book Co., Inc., New York, 1956), p. 406.

[10] Timoshenko, S. and Woinowsky-Krieger, S., *Theory of Plates and Shells* (McGraw-Hill Book Co., Inc., New York, 1957).

[11] Stowell, E. Z., "A unified theory of plastic buckling of columns and plates," NACA TR 898 (1948).

MARCH-APRIL J. AIRCRAFT VOL. 3, NO. 2

An Investigation of Catalytic Ignition of JP-5 and Air Mixtures

Stephen E. Grenleski* and Felix Falk†

Applied Physics Laboratory, The Johns Hopkins University, Silver Spring, Md.

An experimental investigation of the ignition of JP-5 and air mixtures by platinum catalysts was made using sectional and large-scale ramjet engine baffle combustors. Ignition delay data are presented for combustion chamber static pressures of 0.5 to 9.0 atm, inlet air total temperatures of 580° to 1280°F, and fuel-air ratios of 0.007 to 0.09. A thermal model is used to explain the igniter operation.

Introduction

Ignition of the fuel-air mixtures at various pressures and temperatures is one of many problem areas encountered in ramjet combustor development. Experiments conducted by the General Electric Company,[1] in which platinum was used as an igniter in the afterburner of gas turbine engines, aroused interest in the application of platinum igniters to ramjet engines.

The purpose of this paper is to present the results of an investigation which applies the catalysis of JP-5 and air mixtures by platinum (for ignition and oxidation) to ramjet engine baffle combustors and test conditions.

Received May 27, 1965; revision received November 15, 1965. This work was supported by the U. S. Bureau of Naval Weapons under Contract NOw 62-0604-c. The authors wish to acknowledge the encouragement of W. B. Shippen of the Applied Physics Laboratory (APL) and the assistance of J. Funk and E. Taylor (APL) and J. Tucker of the Ordnance Aerophysics Laboratory (OAL) during this program.

* Engineer, Hypersonic Propulsion Group.

† Chemist, Propulsion Engineering Group. Member AIAA.

Experimental Results

This investigation of catalytic ignition of JP-5 and air mixtures was carried out in two distinct phases: first as sectional

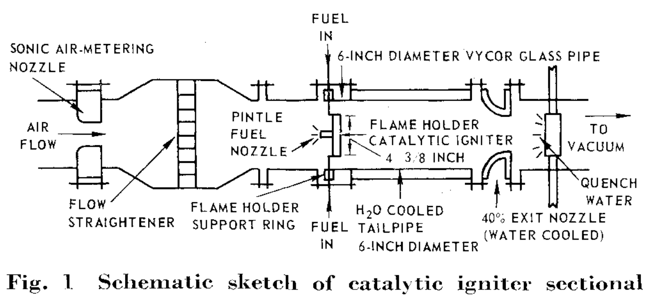

Fig. 1 Schematic sketch of catalytic igniter sectional test setup.